

Working for the betterment of simultaneous deletion of paraben dyes from industrial effluents on to *Origanum majorana*-capped silver nanoparticles

Nima Karachi^{a,*}, Sirous Motahari^b, Saina Nazarian^a

^aDepartment of Chemistry, Marvdasht Branch, Islamic Azad University, Marvdasht, Iran, emails: nimakarachi@miau.ac.ir (N. Karachi), sainanzrian@yahoo.com (S. Nazarian)

^bChemical Engineering Department, Faculty of Science, Yasouj University, Yasouj, Iran, email: sirousmotahari@gmail.com

Received 11 June 2020; Accepted 10 March 2021

ABSTRACT

The applicability of the synthesized *Origanum majorana*-capped silver nanoparticles for eliminating dyes from aqueous media has been confirmed. Identical techniques including Fourier-transform infrared spectroscopy, Brunauer–Emmett–Teller, energy-dispersive X-ray spectroscopy, X-ray diffraction, transmission electron microscopy and scanning electron microscopy has been utilized to characterize this novel material. The investigation showed the applicability of *Origanum majorana*-AgNPs as an available, suitable and low-cost adsorbent for proper deletion of ethylparaben, methylparaben and propylparaben dyes from aqueous media. The optimal conditions for the paraben dyes removal were found to be 7, 65 min, 100 mg L⁻¹, and 50 mg for pH, contact time and adsorbent dosage, respectively. To evaluate the mechanism of adsorption, the kinetic of adsorption process followed second-order equation model. The adsorption mechanism was found fit the second-order ($k_2 = 40.0, 20.6$ and 30.05 g mg⁻¹ min⁻¹ for methylparaben, ethylparaben and propylparaben dyes and $R^2 = 0.98$). After using various isotherm models to fit the experimental equilibrium data with, the adequacy and applicability of Langmuir model has been proven. Thermodynamic parameters of free energy (ΔG°), enthalpy (ΔH°) and entropy (ΔS°) of adsorption were determined using isotherms. The fact that the sorption process was exothermic was the negative value of ($\Delta G^\circ, \Delta H^\circ$ and ΔS°) which on its own expressed the affinity of *Origanum majorana*-AgNPs for removal ethylparaben, methylparaben and propylparaben. The maximum monolayer capacity (q_{max}) was observed to be 30.0, 66.6 and 93.0 mg g⁻¹ for methylparaben, ethylparaben and propylparaben dyes at desired conditions.

Keywords: Adsorption; Paraben dyes; *Origanum majorana*-AgNPs; Isotherms; Thermodynamic

1. Introduction

Parabens as a series of p-hydroxybenzoates acid are synthetic chemicals utilized as preservatives and antimicrobial in a diverse products especially personal care products, pharmaceutical, food [1], beverages and industrial. The application of parabens in toothpastes, sunscreen creams, glues, cosmetics, fats and oils is inevitable. The antifungal and antibacterial properties of parabens and their positive human safety profile can justify their vast

application [2,3]. In some reports it was declared that parabens can spur the growth of certain forms of breast cancer [4] and melanoma in younger people [5] if applied for a long time. Also some male reproductive disorders in a few published studies have been associated to high concentrations of parabens [6]. Thanks to all aforementioned applications of parabens, they found their path to municipal sewage systems. Eliminating parabens by some wastewater treatment technologies is possible [7]. However, small amounts of parabens (at low ng L⁻¹ level) have been spotted

* Corresponding author.

in river water samples [8]. In addition, the appearance of parabens in soil and sediment samples has drawn the attention of environmentalists [9].

Adsorption is one of the best and simple techniques for the removal of toxic and noxious impurities in comparison to other conventional protocols like chemical coagulation, ion exchange, electrolysis, biological treatments is related to advantages viz. lower waste, higher efficiency and simple and mild operational conditions. Adsorption techniques also have more efficiency in the removal of pollutants which are highly stable in biological degradation process through economically feasible mild pathways [10–12]. Thus, the extensive utilization of adsorption techniques for deletion of numerous chemicals from aqueous solutions seems logical [13]. For deletion of dyes pollutants, nanomaterial's based adsorbents are highly proposed [14,15]. Physical and chemical properties of the adsorbent are determinative in efficient applicability of an adsorption process. Among the essential properties of an adsorbent, high adsorption capacity, recoverability and availability at economical cost are mentionable. Nowadays, diverse potential adsorbents have been used for deletion of specified organics from water samples. From this perspective, an extensive survey was conducted on magnetic nanoparticles as novel adsorbents with high adsorption capacity, large surface area, and small diffusion resistance. As an instance, for dissociation of chemical species like environmental pollutants, metals, dyes, and gases, magnetic nanoparticles were used [16,17]. Specifically the application of colorimetric sensors equipped with silver nanoparticles (AgNPs) has drawn the attentions owing to their unique optical properties and localized surface plasmon resonance absorption [18]. Additionally, the confirmed antimicrobial characteristics of Ag^+ ions led to the extensive application of AgNPs. Therefore, AgNPs have been utilized in the fields of pharmacy, nanomedicine, biomedical engineering and biosensing thanks to their exclusive properties [19]. The surface functionalization and stabilization of AgNPs is crucial in sensing metal ions [20].

In this current study, after synthesizing *Origanum majorana*-capped silver nanoparticles as a unique adsorbent, its characterization by Fourier-transform infrared spectroscopy (FT-IR), scanning electron microscopy (SEM), and X-ray diffraction (XRD) analysis has been carried out. In the process of methylparaben, ethylparaben and propylparaben dyes deletion, the effects of important variables like contact time, pH of solution, adsorbent dosage and initial ions concentration as well as the dyes deletion percentage as response were investigated and optimized. The fact that the pseudo-second-order rate equation matched the adsorption of propylparaben was evident. Also the Langmuir model could get better of other models in explaining the equilibrium data. However specific isotherm models viz, Freundlich, Langmuir, Dubinin–Radushkevich and Temkin were used to fit the experimental equilibrium data. But eventually the findings confirmed the suitability and applicability of the Langmuir model. Moreover, it was shown that the kinetic of adsorption process between the kinetic models of pseudo-first-order and pseudo-second-order diffusion models was under the control of the latter one. The success of the *Origanum majorana*-AgNPs in deleting the dyes effectively was proven. The sentences of this paragraph should

be written in the future tense and most of this paragraph sentence should be written in the results section and conclusion. Therefore, the *Origanum majorana*-capped silver nanoparticles will be prepared, characterized and used as a unique adsorbent for removal of paraben dyes from aqueous solutions in this work. Moreover, factors affecting the adsorption are along with the kinetic and isotherm parameter will be investigated.

2. Experimental

2.1. Instrumentation

By utilizing a Maya Pro 180 spectrophotometer (Shimadzu Company, Japan), UV-Visible spectra were measured at ambient temperature. Through the instrumentality of a PerkinElmer (FT-IR spectrum BX, Germany), the record of FT-IR spectra was done. The morphology of samples went through a phase of A detailed examination using scanning electron microscopy (SEM: KYKY-EM 3200, Hitachi Company, China) under an acceleration voltage of 26 kV). On a JEOL 3010, TEM images (transmission electron microscopy images) were registered. For measuring the pH, pH/Ion meter (model-728, Metrohm Company, Switzerland) was employed. All night long, the laboratory glassware was left to soak in 10% nitric acid solution [21].

2.2. Reagents and materials

All chemicals comprising of methylparaben, propylparaben and ethylparaben dyes, silver nitrate (AgNO_3), sodium hydroxide, hydrochloric acid in their pure form were provided from Merck & Co. (Darmstadt, Germany). The preparation of the stock solution (100 mg L^{-1}) of paraben dyes was as follows: 10 mg of solid dye was dissolved in 100 mL double distilled water.

2.3. Synthesis of *Origanum majorana*-capped AgNPs

The successful application of silver nanomaterials in different dimensions and forms in a wide variety of fields including medical, engineering (electric devices), art (painting), and health (cleaning products like soap, detergents) has drawn the attentions [22]. Therefore, in order to take measures in optimizing the use of silver nanomaterials in these applications, knowing their specific physical, chemical and optical properties of them is of great importance. In that connection, comprehensive knowledge of details of the materials (surface property, apparent morphology, size distribution, dissolution rate particle composition) is vital in their synthesis. Based on the method in the literature, the preparation of *Origanum majorana*-capped AgNPs was carried out by reduction of AgNO_3 as a modifier [22]. Simply put, with the help of a reaction flask, 10.0 mL of *Origanum majorana* (0.1 mM) solution and 90.0 mL of AgNO_3 (0.1 mM) solution were blended and stirred vigorously. The above solution was agitated for 1 h. After 15 min, UV-Visible spectrum of *Origanum majorana*-capped AgNPs was provided and inset picture of *Origanum majorana*-capped AgNPs was examined. The color-shifting of the colloidal solution from dark to bright yellow provided the proof for the formation

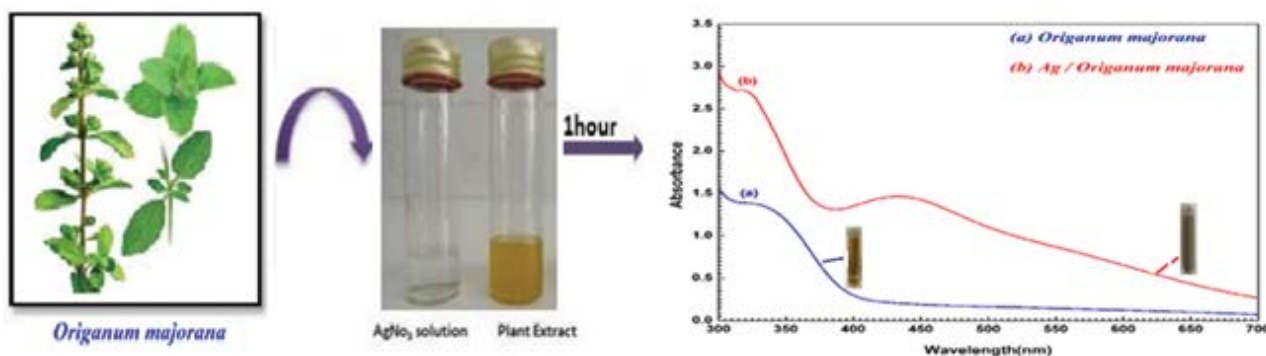


Fig. 1. Synthesis of *Origanum majorana*-capped AgNPs.

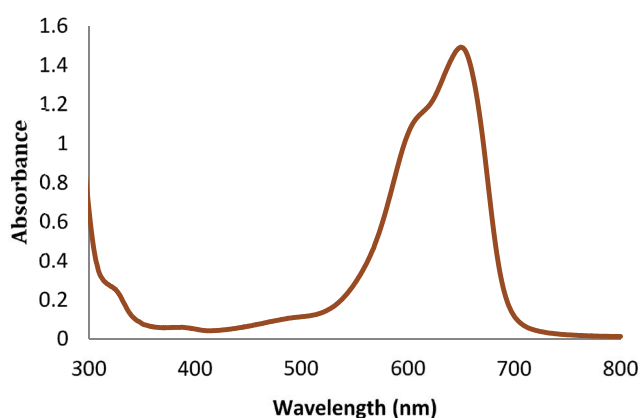


Fig. 2. Physisorption isotherm of *Origanum majorana*-capped silver nanoparticles.

of *Origanum majorana*-capped AgNPs. In order to guarantee the stability of the *Origanum majorana*-capped AgNPs solution for several weeks, it was stored at $4.0^{\circ}\text{C} \pm 2.0^{\circ}\text{C}$ in the absence of light. This paragraph should be written in the correct and clear form, many double spaces between words should be removed, AgNO_3 should be changed to AgNO_3 and space between AgNO_3 and (0.1 mM) should be added.

2.4. Batch adsorption dyes adsorption process

To ascertain the paraben dyes adsorption isotherm onto *Origanum majorana*-capped silver nanoparticles and also to determine its kinetic properties, batch adsorption tests were executed. First, 500 mL solution containing 100 mg L^{-1} concentration of paraben dyes was provided. When adjustment of initial pH of the solution was done by 0.01 NH_4Cl /0.01 N NaOH aqueous solution, no further adjustments were performed in the course of the trials. By dividing this 500 mL solution into ten samples of 50 mL, ten flasks (100 mL) with fixed adsorbent dose of 100 mg L^{-1} were provided. With the help of an orbital shaker, these flasks were agitated at a steady rate of 200 rpm and controlled temperature of 25°C . At fixed time intervals, one flask was withdrawn from orbital shaker (10–80 min) and the analysis of the remaining dyes in the sorbate solution was performed. With the aid of Whatman No. 42 filter paper, *Origanum majorana*-AgNPs were filtered

from aqueous solution. The measurement of paraben dyes concentration in the solution was carried out a double beam UV-Visible spectra were measured utilizing a Maya Pro 180 spectrophotometer (Shimadzu Company, Japan) set at wavelengths 680 nm. The calculation of the quantity of adsorbed dyes at equilibrium (q_e , mg g^{-1}) was done employing the ensuing equation:

$$\% \text{dye} = \frac{(C_0 - C_t)}{C_0} \times 100 \quad (1)$$

where C_0 (mg L^{-1}) refers to the concentration of target at initial time t and C_t (mg L^{-1}) stands for the concentration of target after time t .

$$q_e = \frac{(C_0 - C_e)}{W} \quad (2)$$

In the above equation Q refers to the quantity of dyes adsorbed onto unit quantity of sorbent (mg g^{-1}); C_0 demonstrates the concentrations (mg mL^{-1}) of dyes in the primary solution and the concentrations of dyes in the aqueous phase after adsorption is demonstrated by C . The volume of the aqueous phase (mL) is shown by V ; and w shows the weight of the sorbent (g). The evaluation of the thermodynamic properties of the adsorption process was performed by adding 50 mg of *Origanum majorana*-AgNPs into 50 mL initial paraben dyes concentration ranging from 100 mg L^{-1} the PH was adjusted to 7.0 as the optimum value, in each experiment. For 65 min and at 25°C , each solution was shaken uninterruptedly. The paraben dyes concentration were estimated after the solution equilibrium and desorption outcomes were obtained in the present work [23]. Then with the help of a UV-Vis spectrophotometer which was adjusted at wavelength of 680 nm, non-adsorbed dye contents were determined for paraben dyes.

3. Findings and discussion

3.1. Characterization of adsorbent

The nitrogen adsorption–desorption isotherm at 77 K onto *Origanum majorana*-capped silver nanoparticles has been presented in Fig. 3. This isotherm is consistent with

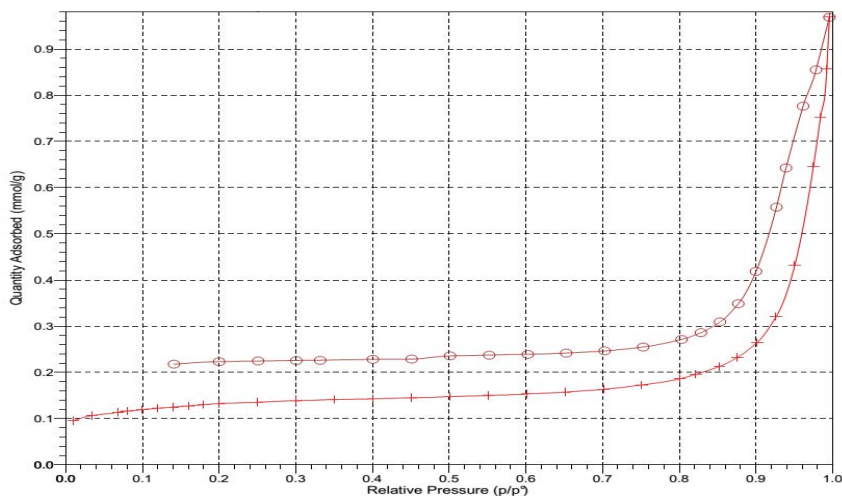


Fig. 3. Physisorption isotherm of *Origanum majorana*-capped silver nanoparticles.

classical type III isotherm of IUPAC classification [24]. The porosity and chemical reactivity of functional groups at the surface control the adsorption capacity of *Origanum majorana*-capped AgNPs. Comprehensive Knowledge of the surface functional groups would provide an overview of the adsorption potentiality of the *Origanum majorana*-capped AgNPs.

Fig. 4 clearly shows the FT-IR spectrum of *Origanum majorana*-capped AgNPs nanoparticles loaded on activated carbon. The wide signals at ≤ 900 and $1,048$ in Ag–O, $1,386$ – $1,422$ cm^{-1} are ascribable to C–H stretching from *Origanum majorana*-capped AgNPs, and the ones at $1,634$ cm^{-1} to C=O bonds. The appeared signal at $2,027$ cm^{-1} is relative to C–H stretching while the one at $3,412$ cm^{-1} is attributed to –OH stretching [25]. Energy-dispersive X-ray spectroscopy (EDX) spectrum of (a) The EDX transmittance spectrum

of the prepared *Origanum majorana* and (b) EDX spectrum recorded from a film, after formation of silver nanoparticles. Different X-ray emission peaks are *Origanum majorana*-capped silver nanoparticles Fig. 5 [26]. The adsorption of paraben dyes and based on Fig. 6a which is the XRD pattern of the *Origanum majorana*-capped AgNPs, the signals at 38.07 (111), 44.26 (200), 64.43 (220) and 77.35 (311) are ascribable to diffractions and reflections from the carbon atoms [27]. Obviously the perfect crystalline nature of the material was proven after functionalizing with *Origanum majorana*-capped AgNPs however the great intensity of signal at 38.07 (111) confirmed that there has been a slight amount of material in amorphous state. The perfect synthesis of *Origanum majorana*-capped AgNPs is obvious through looking at XRD pattern. In Figs. 6a and b, the image TEM of the prepared *Origanum majorana*-capped AgNPs the

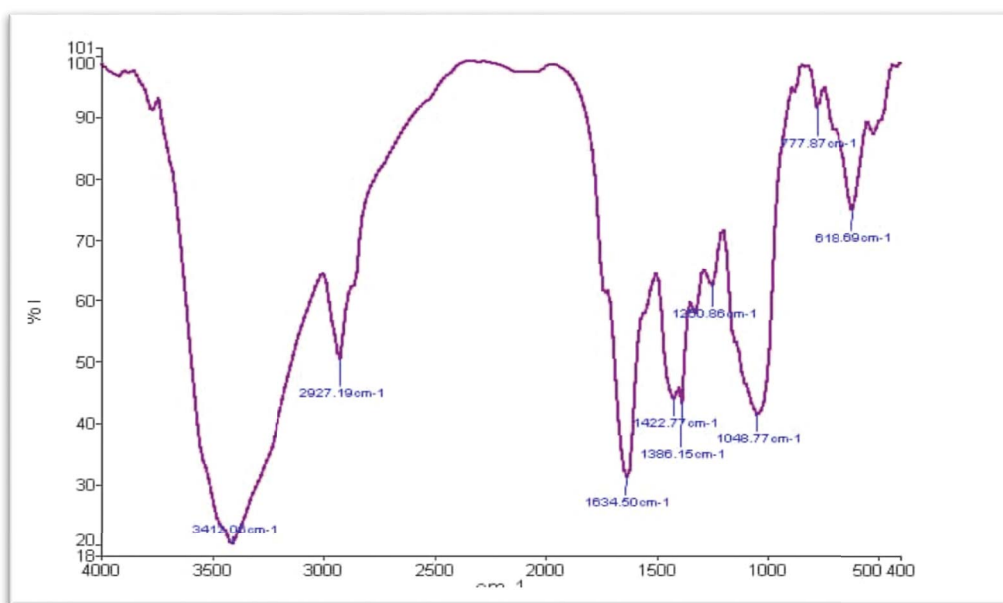


Fig. 4. FT-IR transmittance spectrum of the prepared *Origanum majorana*-capped AgNPs.

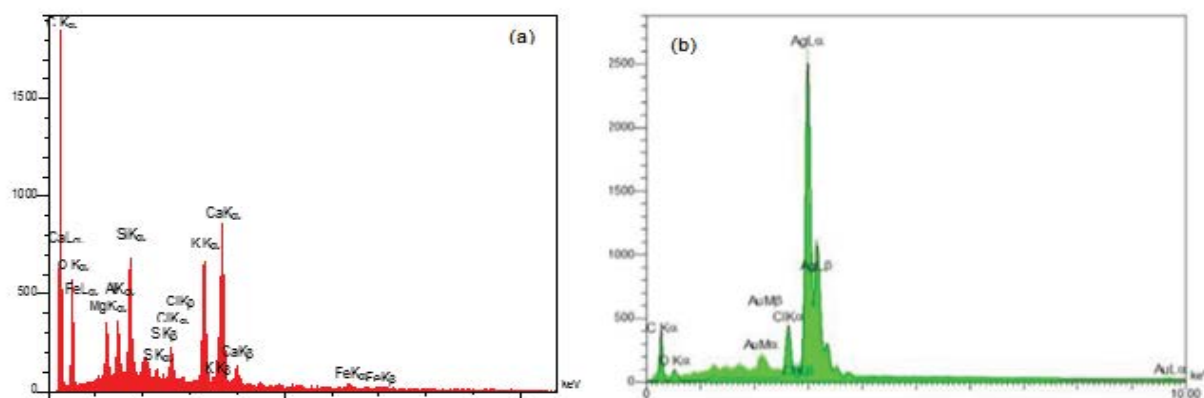


Fig. 5. (a) EDX transmittance spectrum of the prepared *Origanum majorana* and (b) EDX spectrum recorded from a film, after formation of silver nanoparticles. Different X-ray emission peaks are *Origanum majorana*-capped silver nanoparticles.

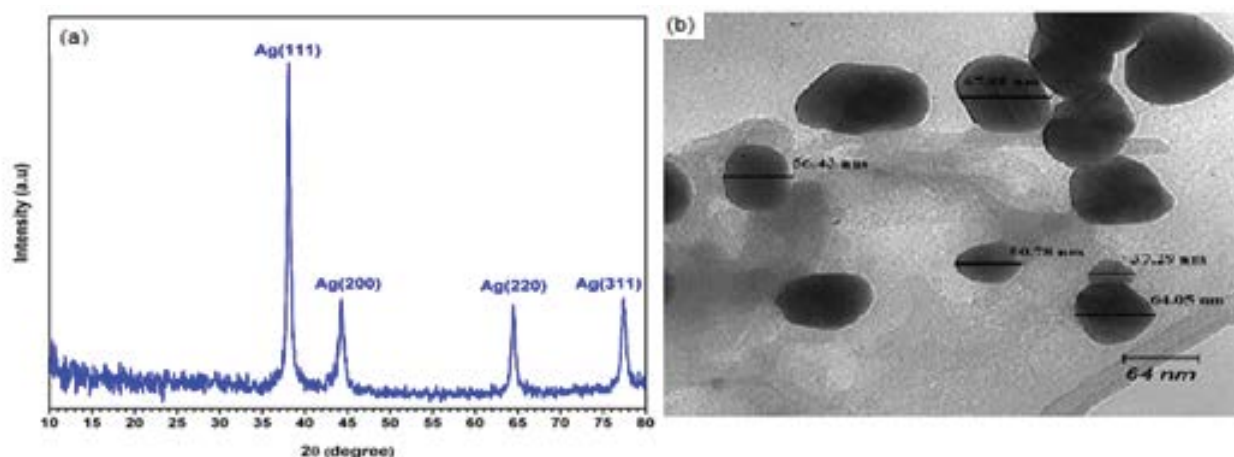


Fig. 6. (a) XRD image and (b) TEM of the prepared *Origanum majorana*-capped AgNPs.

morphological properties of the samples scrutinized by SEM are exhibited. By looking at Fig. 7, the smoothness, homogeneity and tidiness of *Origanum majorana*-capped AgNPs are confirmed. Even uniformity size distribution is observable in Fig. 7. After surface modification, the *Origanum majorana*-capped AgNPs became uneven, larger and bundled [28].

3.2. Impact of pH on the adsorption

The impact of pH value in the adsorption process is significant. In Fig. 8 the deletion of ethylparaben, methylparaben and propylparaben dyes as a function of pH at different sorbent is presented. To control desired pH for the highest deletion of dyes, the measurement of equilibrium adsorption of paraben dyes was done at diverse pH levels from 4.0 to 10.0 through adjusting the initial ethylparaben, methylparaben and propylparaben dyes concentrations at 10 ppm and the summary of the outcomes are recorded in Fig. 8 [29]. At pH = 7.0, *Origanum majorana*-capped silver nanoparticles provided the highest deletion percentages of ethylparaben, methylparaben and propylparaben dyes as follows: for methylparaben it was 78.3%, for ethylparaben 80.4% and for propylparaben was 87.4%.

Any abatement in dyes deletion at basic pH ($\text{pH} < 7$) for paraben is due to the competition of ethylparaben, methylparaben and propylparaben dyes with H^+ . However again, in a very acidic pH, protonation of nitrogen atoms on the surface of adsorbents due to the high concentration of H^+ can reduce any interaction with paraben dyes and surface of adsorbents. Any abatement in paraben dyes deletion at $\text{pH} > 7$ can be related to precipitation of hydroxide and conversion of paraben dyes. Due to this phenomenon, any access of paraben dyes molecules to adsorption sites is obstructed and the consequence will be less adsorption of ethylparaben, methylparaben and propylparaben dyes [30].

3.3. Point of zero charge (PZC)

PZC could directly lead to a qualitative assessment of the type of interactions (attraction or interaction) between *Origanum majorana*-AgNPs if we know the type of charges on their surfaces. Unfortunately, it is experimentally difficult to directly measure the charges on the surface. Instead, indirect methods are available such as estimation of PZC from electrochemical impedance spectroscopy measurement. PZC is an expedient marker of surface charges, that is critically relevant to adsorption of an electrolyte. It denotes

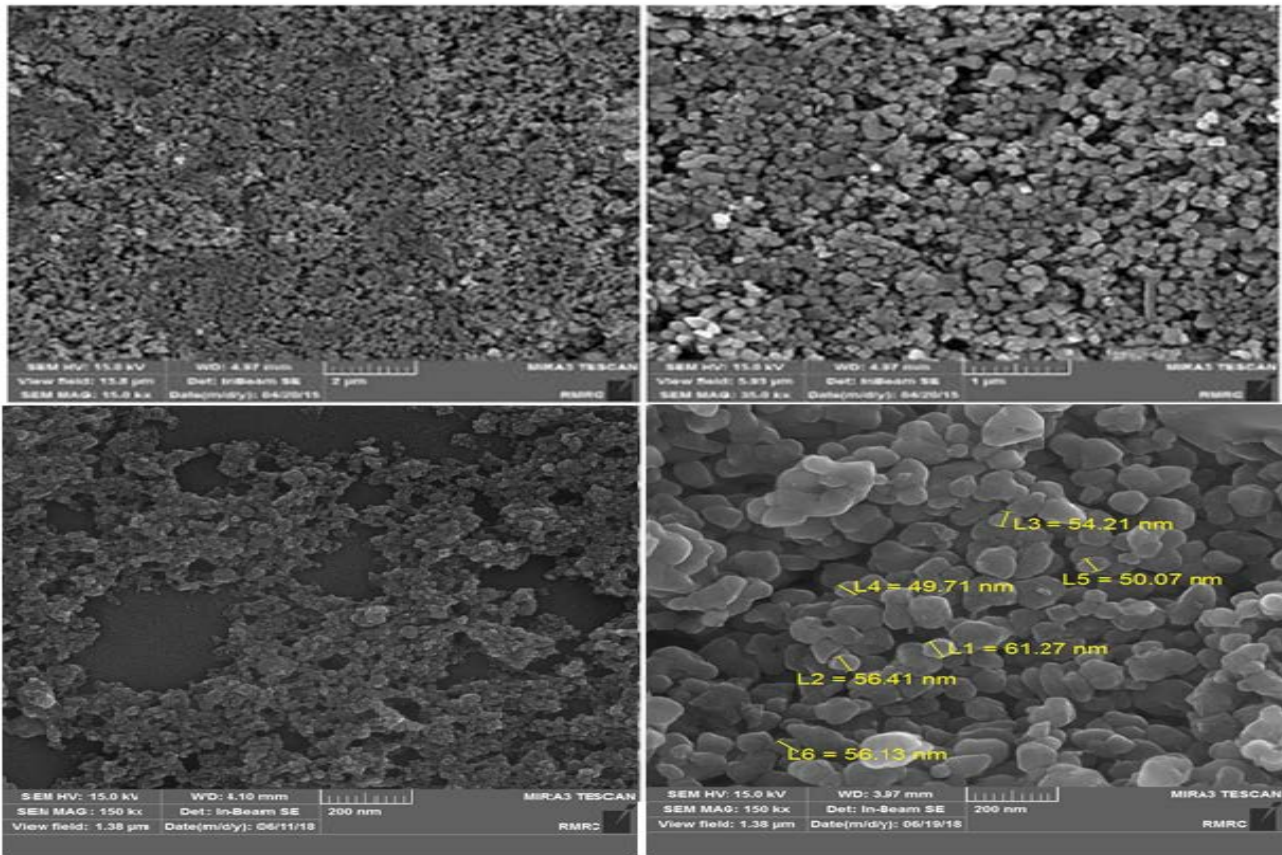


Fig. 7. SEM image of the prepared *Origanum majorana*-capped AgNPs.

the potential when the surface carries zero charges. Normally, when electrode potential is larger than PZC, the electrode carries positive charges and when it is smaller than PZC, the electrode carries negative charges. The pH value of the solution, affects the surface charge of the adsorbent and the uptake behavior and efficiency of adsorbent [31].

3.4. Impact of the dosage of biosorbent

Since biosorbent dosage determines the capacity of a biosorbent for a given initial ions concentration, it is recognized as an important parameter. Therefore, a thorough investigation was performed on the biosorption efficiency for paraben dyes as a function of biosorbent dosage. Based on what is observed in Fig. 10, the percentage of the dyes biosorption rose sharply when the biosorbent charged to 50 mg. This finding is explainable in this way that while the biosorption sites remained unsaturated in the course of the biosorption reaction, the number of available sites for biosorption grew greater by enhancing the biosorbent dose [32]. The highest biosorption was achieved at biosorbent dosage of 50 mg. Thus, 50 mg was selected as the preferred biosorbent dosage for further experiments. This fact is explainable in another way that small biosorbent ratio results in less active sites for binding metal ions on the surface of *Origanum majorana*-capped AgNPs and therefore the biosorption efficiency is low. Upon any increase in the biosorbent dose, more active sites are provided to

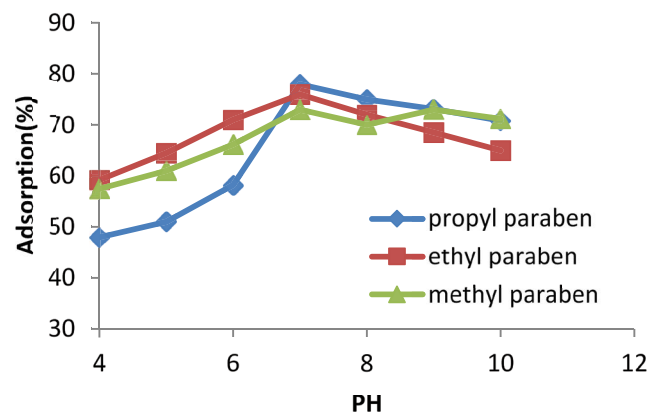


Fig. 8. Impact of pH on paraben dyes deletion [paraben dyes conc. = 100 mg L⁻¹; contact time = 65 min; adsorbent dose = 50 mg; stirring speed = 180 rpm; temp. = 25°C].

bind with paraben dyes which provokes an increase in the biosorption efficiency until saturation.

3.5. Impact of the contact time on the adsorption

Fig. 11 displays the impact of contact time on sorption of paraben dyes by synthesized *Origanum majorana*-AgNPs. It can be spotted that a little alteration in sorption rate at 65 min onto *Origanum majorana*-AgNPs happened

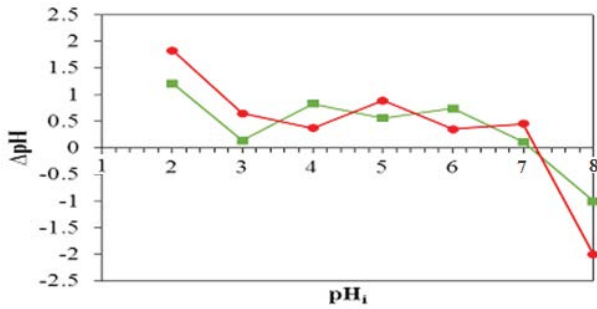


Fig. 9. Impact of pH on paraben dyes deletion [paraben dyes conc. = 100 mg L⁻¹; contact time = 65 min; adsorbent dose = 50 mg; stirring speed = 180 rpm; temp. = 25°C].

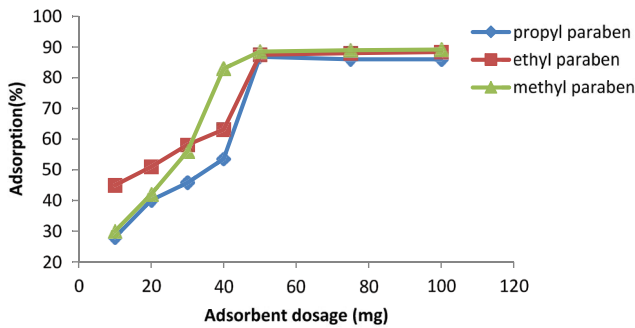


Fig. 10. Impact of the dosage of adsorbent on paraben dyes deletion [paraben dyes conc. = 100 mg L⁻¹; pH = 7.0; stirring speed = 180 rpm; contact time = 60 min; temp. = 25°C].

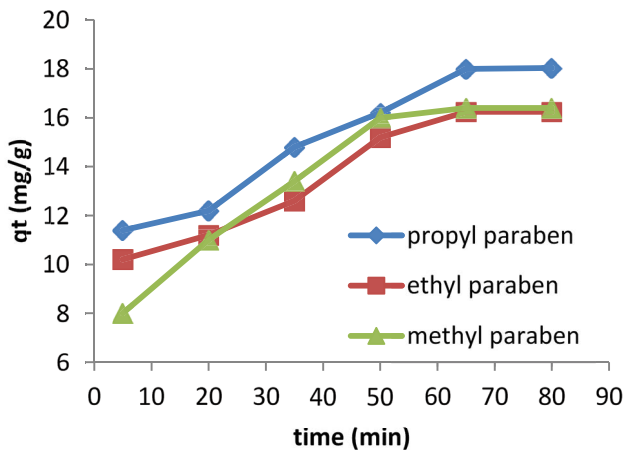


Fig. 11. Impact of time on paraben dyes deletion [paraben dyes conc. = 100 mg L⁻¹; pH = 7.0; contact dose adsorbent = 50 mg; stirring speed = 180 rpm; temp. = 25°C].

and then slowly leveled off till no noticeable increasing in the adsorption of paraben dyes was observed and the deletion finally reached equilibrium [33]. Thus, the percentages of 79.0%, 88.1% and 73.5% were recorded as the highest removal percentages for ethylparaben, methylparaben and propylparaben dyes at contact time 65 min onto *Origanum majorana*-AgNPs, respectively.

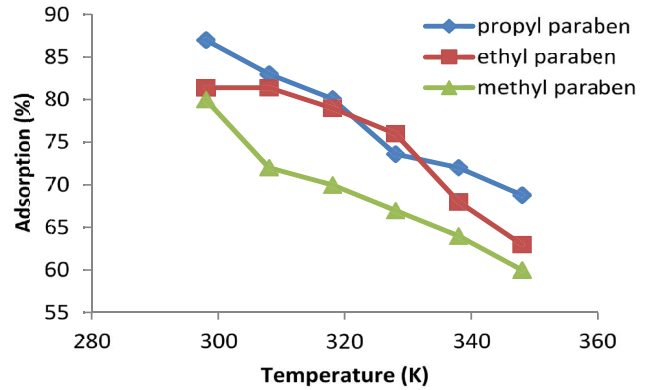


Fig. 12. Impact of temperature on paraben dyes deletion [paraben dyes conc. = 100 mg L⁻¹; adsorbent dose = 50 mg; pH = 7.0; stirring speed = 180 rpm; contact time = 60 min].

3.6. Impact of temperature

Fig. 12 displays the impact of temperature on the adsorption of paraben dyes. From the results it is evident that there is a gradual increase in the adsorption of methylparaben dyes from 60.0% to 80.0% and for ethylparaben dyes from 60.0% to 80.0% and for propylparaben dyes from 59.0% to 76.0% onto *Origanum majorana*-AgNPs. The endothermicity of the adsorption was proven by the foregoing outcomes. By considering the porosity nature of the adsorbent and the likelihood of diffusion of adsorbate thus, sorption will increase with the rise of temperature that affects the diffusion. In addition, as the process is endothermic, the rise in temperature works for the benefit of the adsorbate transport within the pores of adsorbent [34].

3.7. Biosorption isotherms

The subdivision of sorbate molecules that are subdivided between liquid and solid phases at equilibrium is described by adsorption isotherm. Under the auspices of four adsorption isotherms of Freundlich, Langmuir, Temkin, and Dubinin–Radushkevich isotherms, adsorption of paraben dyes onto *Origanum majorana*-capped silver nanoparticles was modeled [35].

The equilibrium relationship premised on mathematical connection of an established equilibrium between the amount of adsorbed target per gram of adsorbent (q_e , mg g⁻¹) to the equilibrium non-adsorbed quantity of dyes in solution (C_e , mg L⁻¹) at specified temperature is defined by adsorption equilibrium isotherms [36,37]. Under the auspices of 3 models of Freundlich adsorption isotherm, Langmuir adsorption isotherm and Dubinin–Radushkevich isotherms, the adsorption isotherm of adsorption was scrutinized.

- Based on Langmuir adsorption isotherm model: no interaction existed amongst adsorbed molecules and adsorption process on uniform surfaces. The ensuing equation presents Langmuir model [38]:

$$\frac{C_e}{q_e} = \frac{1}{K_L q_{max}} + \frac{C_e}{q_{max}} \quad (3)$$

In the foregoing equation, the equilibrium concentration, the adsorption capacity and the maximum adsorption capacity of the adsorbents in the aqueous medium are shown by C_e (mg L^{-1}), q_e (mg g^{-1}) and q_{max} (mg g^{-1}) respectively. K_L as a constant is associated with binding energy of the sorption system (L mg^{-1}) (Fig. 13a).

- Freundlich adsorption isotherm defines the multilayer adsorption of an adsorbate onto a non-uniform surface of an adsorbent. The ensuing equation introduces the linear form of Freundlich isotherm model:

$$\log q_e = \log K_F + \frac{1}{n} \log C_e \quad (4)$$

The Freundlich isotherm constants are the K_F (the adsorption capacity) and n (intensity of a given adsorbent) (Fig. 13b).

As shown in Figs. 12b and c, for the both models, the slope and the position of the constant determined their values. Table 1 displays the outcomes of the fit and of the constants of both models for paraben dyes. The values of n for MP, EP and PP dyes onto *Origanum majorana*-AgNPs were 9.42, 9.37 and 9.97, respectively. The desired value for n in the adsorption process was between 1 and 10 [39]. The Langmuir isotherm was confirmed to be the perfect model to demonstrate the adsorption of dyes onto *Origanum majorana*-AgNPs adsorbent if considering all the correlation coefficients and parameters procured for the isotherm models (Table 1).

- In Temkin isotherm equation, there exists a presumption that the heat of biosorption of all the molecules in the layer reduces linearly with coverage owing to adsorbent–adsorbate interactions. And also it is presumed that the adsorption is characterized by a uniform distribution of the binding energies up to some top binding energy [39]. The ensuing introduces the linear form of the Temkin isotherm:

$$\log \left(\frac{1}{q_e} \right) = \log \left(\frac{k_L + 1}{k_L q_m} \right) + \frac{1}{n} \log \left(\frac{1}{C_e} \right) \quad (5)$$

In Fig. 13c: the plots of $\ln(C_e)$ vs. q_e for ethylparaben, methylparaben and propylparaben dyes are exhibited. The summary of the linear isotherm parameters b_T , K_T and the correlation coefficient are displayed in Table 1. The b_T constant corresponding to heat of sorption for methylparaben, ethylparaben and propylparaben dyes onto *Origanum majorana*-capped silver nanoparticles adsorbent equals $21.441 \text{ J mol}^{-1}$.

- To analyze the nature of adsorption, Dubinin–Radushkevich isotherm model is utilized. In the ensuing equation, the linear form of this model is introduced:

$$\ln q_e = \ln q_m - \beta \epsilon^2 \quad (6)$$

where β in the above equation refers to the activity coefficient corresponding to mean sorption energy (mol^2/kJ^2), and

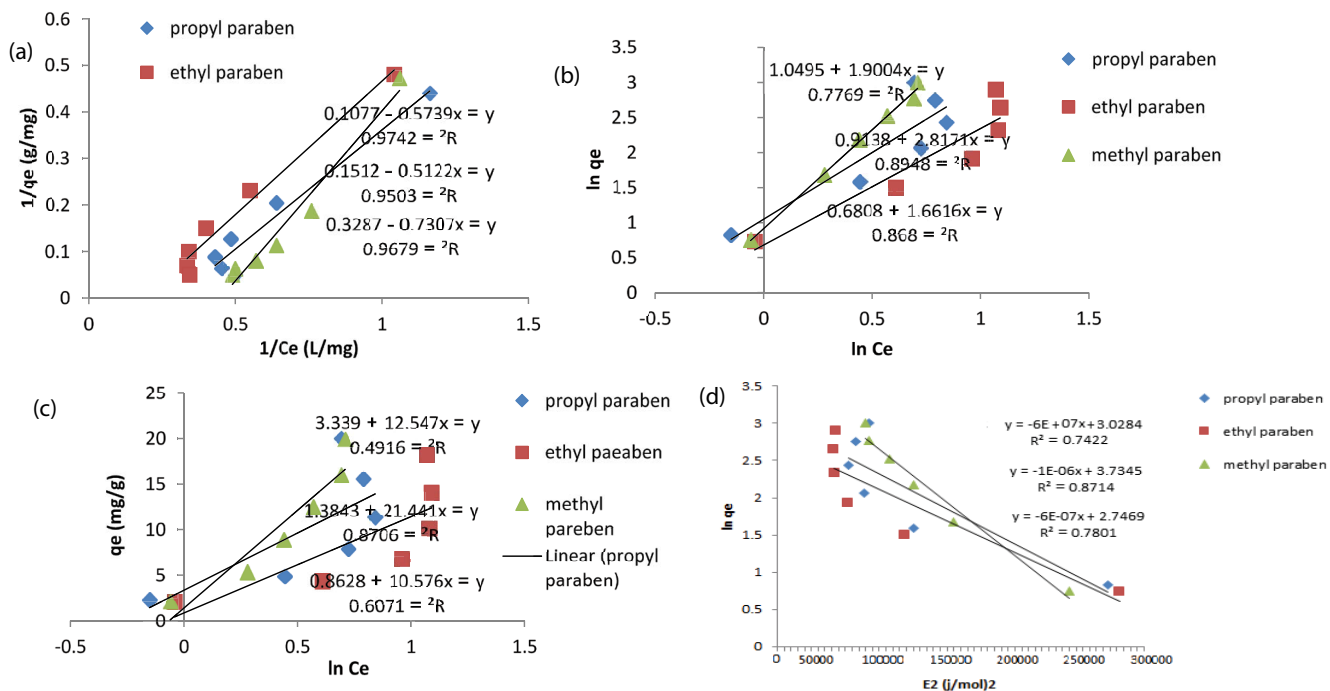


Fig. 13. (a) Langmuir isotherm for the adsorption of paraben dyes [pH = 7.0; adsorbents dose = 50 mg; temp. = 25°C]. (b) Adsorption of propylparaben dyes [initial paraben dyes = 100 mg L^{-1} ; pH = 7.0; adsorbents dose = 50 mg; temp. = 25°C] based on Freundlich isotherm. (c) Temkin isotherm for the adsorption of paraben dyes [initial paraben dyes conc. = 100 mg L^{-1} ; pH = 7.0; adsorbents dose = 50 mg; temp. = 25°C]. (d) Dubinin–Radushkevich isotherm for the adsorption of paraben dyes [initial paraben dyes conc. = 100 mg L^{-1} ; pH = 7.0; adsorbents dose = 50 mg; temp. = 25°C].

Table 1
Estimation of different isotherm constants and correlation coefficients for the adsorption of paraben dyes onto *Origanum majorana*-capped silver nanoparticles

Isotherm	Equation	Parameters	Value of parameters for propylparaben dyes	Value of parameters for ethylparaben dyes	Value of parameters for methylparaben dyes
Langmuir	$q_e = \frac{q_m b C_e}{1 + b C_e}$	q_m (mg g ⁻¹)	93.0	66.6	30.0
		K_L (L mg ⁻¹)	0.45	0.3	0.2
		R^2	0.9742	0.9503	0.9679
		n	0.61	0.53	0.4
Freundlich	$\ln q_e = \ln K_f + \frac{1}{n} \ln C_e$	K_f (mg) ¹⁻ⁿ L ⁿ g ⁻¹	2	2.9	2.6
		R^2	0.8948	0.8680	0.7769
		A_T (L mg ⁻¹)	1.1	1.3	1.07
Temkin	$\log\left(\frac{1}{q_e}\right) = \log\left(\frac{k_t + 1}{k_t q_m}\right) + \frac{1}{n} \log \frac{1}{C_e}$	b_T	10.576	12.547	21.441
		R^2	0.8706	0.4916	0.6071
		q_m (mg g ⁻¹)	15.6	20.7	22.0
Dubinin–Radushkevich	$\ln q_e = \ln Q_d - B \epsilon^2$	E (kJ mol ⁻¹)	-903.7	-903.7	-700.0
		R^2	0.7801	0.7422	0.8714

ϵ stands for the Polanyi potential which is calculable by the following equation:

$$\epsilon = RT \ln \left(1 + \frac{1}{C_e} \right) \tag{7}$$

where R stands for the desired gas constant (8.3145 J mol⁻¹ K⁻¹) and T for the absolute temperature (K) (Fig. 12d). The free energy change of adsorption (kJ mol⁻¹) that stands in need of transferring 1 mol of ions from solution to the adsorbent surface is shown by E_a and it is measurable from the ensuing equation [40]:

$$E_a = \frac{1}{(-2\beta)^{1/2}} \tag{8}$$

In this model, the mechanism of adsorption is considered physical if E_a is smaller than 8 kJ mol⁻¹ while if $8 > E_a < 20$ kJ mol⁻¹, the dominancy of chemical ion exchange in the adsorption is confirmed and eventually if E_a is greater than 20 kJ mol⁻¹, the mechanism of paraben dyes adsorption is considered to be chemical [41,42]. The values of E for paraben dyes onto *Origanum majorana*-AgNPs were 1.052, 1.041 and 1.030 respectively.

3.8. Adsorption kinetic surveys

Different parameters relative to both the state of the solid (generally with very non-uniform reactive surface) and physicochemical conditions under which the adsorption is taking place can affect the adsorption in aqueous medium [43]. Four kinetic model of (1) intraparticle diffusion model, (2) Elovich, (3) pseudo-first-order and (4) pseudo-second-order were applied to the data to scrutinize the adsorption kinetics of dyes [44,45]. The adsorption kinetic

data were described by the Lagergren pseudo-first-order model [46]. The following clearly expresses the Lagergren:

$$\frac{dq_t}{dt} = k_1 (q_e - q_t) \tag{9}$$

- The pseudo-first-order model is introduced through the ensuing equation:

$$\ln(q_e - q_t) = \ln q_e - k_1 t \tag{10}$$

where k_1 is the rate constant of adsorption (min⁻¹). The quantities of paraben dyes adsorbed per unit mass of the adsorbent (mg g⁻¹) at equilibrium and time t are shown by q_e and q_t respectively (Fig. 14a). q_e and q_t are calculable by the followings:

- The ensuing equation shows the pseudo-second-order model:

$$\frac{t}{q_t} = \frac{1}{k_{ad} q_e^2} + \frac{1}{q_e} t \tag{11}$$

That k_{ad} stands for the rate constant of equation (g mg⁻¹ min⁻¹) which is calculable from the plots of t/q_t vs. t . Also $h = k_{ad} q_e^2$ (mg g⁻¹ min⁻¹) (Fig. 14b).

- The ensuing formula expresses the Elovich equation:

$$q_t = \frac{\ln(hB)}{B} + \frac{\ln(t)}{B} \tag{12}$$

In the foregoing formula, the desorption constant is shown by β (mg g⁻¹ min⁻¹)

- The ensuing formula introduces the intraparticle diffusion model (Fig. 13d):

Table 2
Comparison of the kinetic parameters for the removal of paraben dyes into *Origanum majorana*-AgNPs

Model	Parameters	Value of parameters for propylparaben dyes	Value of parameters for ethylparaben dyes	Value of parameters for methylparaben dyes
Pseudo-first-order kinetic $\log(q_e - q_t) = \log(q_e) - \left(\frac{k_1}{2.303}\right)t$	$q_{e,cal}$ (mg g ⁻¹)	48.1	56.4	32.9
	k_1 (min ⁻¹)	0.3	0.65	0.4
	R^2	0.9783	0.8331	0.8676
Pseudo-second-order kinetic $\frac{t}{q_t} = \frac{1}{k_2 q_e^2} + \left(\frac{1}{q_e}\right)t$	$q_{e,cal}$ (mg g ⁻¹)	80.94	90.64	90.0
	k_2 (g mg ⁻¹ min ⁻¹)	40.0	20.6	30.05
	R^2	0.9831	0.9891	0.9814
Intraparticle diffusion $q_t = k_{intra}(t)^{1/2} + C$	K_i ((mg g ⁻¹) min ^{-0.5})	0.8212	1.2802	1.0339
	C (Å)	4.8895	5.5043	7.284
	R^2	0.899	0.9497	0.8329
Elovich $q_t = \frac{1}{\beta} \ln(\alpha\beta) + \frac{1}{\beta} \ln(t)$	α (g mg ⁻¹ min ⁻¹)	11.2	6.43	24.42
	β (g mg ⁻¹)	0.53	0.3	0.43
	R^2	0.973	0.957	0.9314

$$q_t = k_{intra}(t)^{1/2} + C \quad (13)$$

where k_{intra} stands for the intraparticle diffusion rate constant (mg g⁻¹ min^{-1/2})

From the slope between q_t vs. $t^{1/2}$, k_{intra} is calculable and C is a constant.

The kinetic model with a greater correlation coefficient R^2 was considered and chosen as the most perfect model. For evaluating the sorption performance of sorbents, k_d must be determined. The following equation is utilized for its calculation:

$$k_d = \left[\frac{C_i - C_e}{C_e} \right] \left(\frac{V}{m} \right) \quad (14)$$

V in the above-mentioned equation shows the solution volume (mL). Higher k_d value is a good indication for being a suitable and successful sorbent in deleting metals.

Table 2 demonstrates the correlation coefficient (R^2) values of the four kinetic models and other calculated, connected kinetic parameters. The appropriateness of the pseudo-second-order kinetic model has been confirmed on the ground of the obtained values of the correlation coefficient (R^2). The pseudo-second-order kinetic model in comparison with other models showed the highest matching with the experimental data in explaining the adsorption mechanism of paraben dyes into *Origanum majorana*-AgNPs (Fig. 13).

3.9. Adsorption thermodynamics

For the adsorption processes, three thermodynamic parameters of (1) Gibbs free energy change (ΔG°), (2) enthalpy change (ΔH°) and (3) entropy change ΔS° were considered. Their computation becomes possible through utilizing the ensuing equations [47]:

$$K_c = \frac{C_A}{C_S} \quad (15)$$

$$\Delta G^\circ = -RT \ln K_{ad} \quad (16)$$

$$\ln K_{ad} = \frac{\Delta H^\circ}{RT} + \frac{\Delta S^\circ}{R} \quad (17)$$

From a plot of $\ln K_c$ against $1/T$, a graph (Fig. 14) is provided. By considering the slope of this graph ΔG° can be acquired. In Table 3, the summary of the thermodynamic parameter outcomes for the adsorption of paraben dyes onto *Origanum majorana*-AgNPs at diverse temperatures is demonstrated.

The estimation of ΔG° values became possible via employing the equation adsorption of paraben dyes. As can be seen in Fig. 14, with any increase in the temperature from 298 to 348 K, a steep reduction in the *Origanum majorana*-AgNPs adsorbent was observed which confirms the exothermicity nature of the process. The values of the thermodynamic parameters (Table 3) [48,49] were computed using the plots. Moreover, the negative value of ΔG° supports the feasibility and spontaneity nature of the process. On the other hand, the negative value of ΔH° strongly affirms the exothermicity nature of the adsorption and the value of ΔS° affirms an alteration in the randomness at the *Origanum majorana*-AgNPs solution interface in the course of the sorption. The conformity of ΔG° values up to -40.0 , -40.95 and -47.6 kJ mol⁻¹ for methylparaben, ethylparaben and propylparaben dyes with those of electrostatic interaction between sorption sites and the paraben dyes (physical adsorption) has been documented. In this present work, the predominance of the physical adsorption mechanism in the sorption process has been confirmed by the obtained ΔG° values for paraben dyes (< -5 kJ mol⁻¹) [50].

3.10. Recycling of the adsorbent

The ability of recovering and reusing of the adsorbent was tested in several steps of adsorption and desorption. The result is shown in Fig. 15. As shown in Fig. 16 of paraben

Table 3
Thermodynamic parameters for the adsorption of paraben dyes onto *Origanum majorana*-AgNPs adsorbent

Paraben dyes (mg L ⁻¹)	T (°K)	K _c	Value of ΔS° (J mol ⁻¹ K ⁻¹)	Value of ΔH° (kJ mol ⁻¹)	Value of ΔG° (kJ mol ⁻¹)
Methylparaben dyes	298	6.7	-47.6	-18.7	-4.71
	308	4.5			-4
	318	4.03			-3.7
	328	2.79			-2.81
	338	2.57			-2.64
	348	2.21			-2.29
Ethylparaben dyes	298	4.38	-40.95	-16.12	-3.66
	308	4.38			-3.78
	318	3.76			-3.5
	328	3.17			-3.15
	338	2.13			-2.12
	348	1.7			-1.54
Propylparaben dyes	298	4	-40.0	-15.0	-3.44
	308	2.6			-2.4
	318	2.33			-2.25
	328	2.03			-1.94
	338	1.87			-1.63
	348	1.5			-1.16

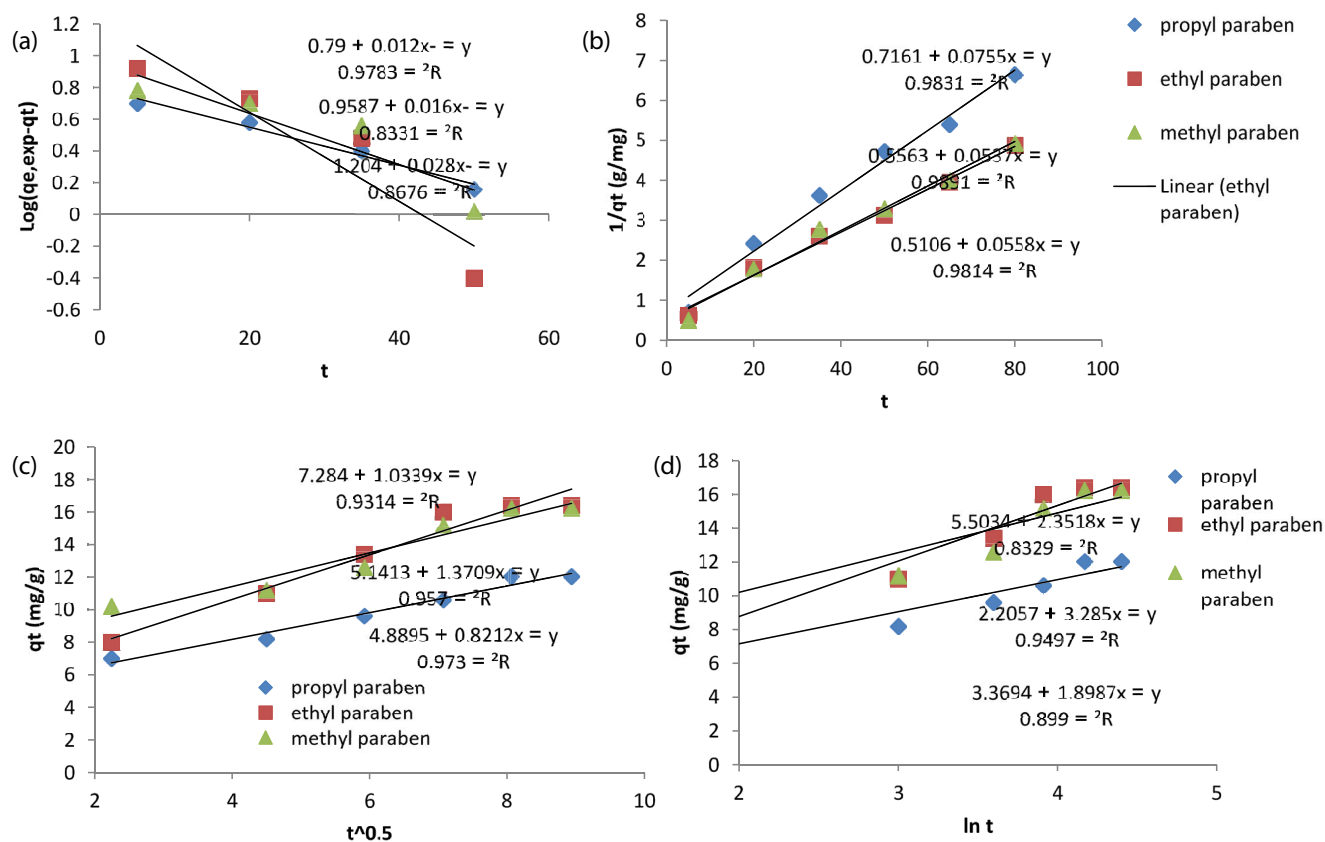


Fig. 14. (a) Pseudo-first-order model for paraben dyes adsorption [initial paraben dyes conc. = 100 mg L⁻¹; contact time = 65 min]. (b) Pseudo-second-order model for paraben dyes adsorption [initial paraben dyes conc. = 100 mg L⁻¹; contact time = 65 min]. (c) Elovich model for paraben dyes adsorption [initial paraben dyes conc. = 100 mg L⁻¹; contact time = 65 min]. (d) Intraparticle diffusion model for paraben dyes adsorption [initial paraben dyes conc. = 100 mg L⁻¹; contact time = 65 min].

dyes was desorbed from the adsorbent after first cycle and after 6 cycles, there were slight changes in paraben dyes desorption. So, it was concluded that the desired removal of 93% can be achieved after 6 cycles.

3.11. Juxtaposition of dyes onto sorbent adsorption method with other

Table 4, demonstrates the max adsorption capacities of varied adsorbents for deletion of dyes comparatively. The type and density of active sites in adsorbents which are responsible for adsorption of metal ions from the solution result in the variation in q_{\max} values. The outcomes of the table clearly show that the sorption capacity of utilized sorbent in the current study is significantly high. In general, morphology, particle size and distribution, and surface structure of this sorbent were effective in its successful outcomes.

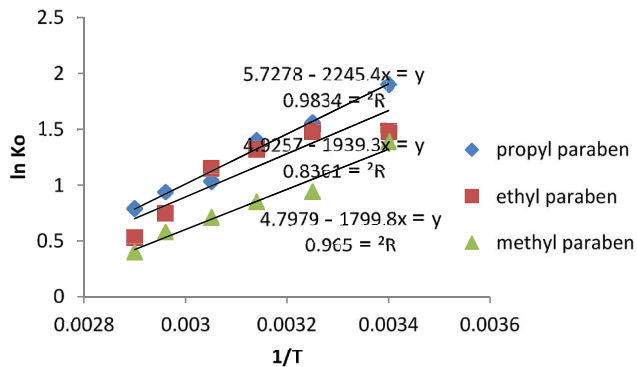


Fig. 15. Plot of $\ln K_c$ vs. $1/T$ for the estimation of thermodynamic parameters.

4. Conclusion

The selection of *Origanum majorana*-capped silver nanoparticles as an efficacious adsorbent for the deletion of paraben dyes from aqueous solutions has been scrutinized. In this current article, the applicability of *Origanum majorana*-AgNPs as an available, useful, and affordable material for deleting paraben dyes from aqueous media has been confirmed. The optimal conditions for the paraben dyes removal were found to be 7, 65 min, 100 mg L⁻¹, and 50 mg for pH, contact time and adsorbent dosage for adsorption of paraben dyes into *Origanum majorana*-AgNPs. Studying the impact of various process parameters revealed that when initial paraben dyes concentration increased, percent adsorption decreased but percent adsorption enhanced when adsorbent dosage enhanced. The highest paraben dyes deletion by the adsorbent occurred at pH 7.0. The maximum adsorption capacities (q_{\max}) were found to be

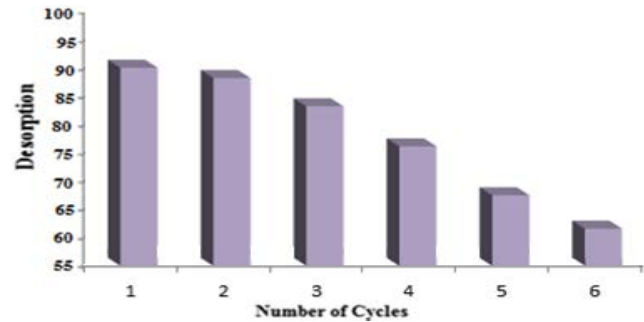


Fig. 16. Desorption of paraben dyes onto *Origanum majorana*-AgNPs [paraben dyes conc. = 100 mg L⁻¹; pH = 7; adsorbent dose = 50 mg; time = 65 min; stirring speed = 180 rpm; temp. = 25°C].

Table 4

Juxtaposition of the adsorption capacities of different adsorbents for the adsorption of removal dyes onto sorbent

Dyes	Adsorbent	Dosage sorbent (g)	Adsorption capacity (mg g ⁻¹)	References
Rhodamine 123 (RH-123) and Disulfine blue (DSB) dyes	Au/Fe ₃ O ₄ NPs nanoparticles loaded on activated carbon	0.025	71.46 and 76.38	[11]
Disulfine blue and Methylene dyes	Titanium dioxide-NPs loaded onto activated carbon	0.25	70.3 and 48.48	[12]
Nitrate	Active carbon magnetic nanoparticles	0.4	57.1	[13]
Orange 122 dye	Fe ₃ O ₄ magnetic nanoparticles	1.4	51.546	[16]
Purpurin dye	Mn-doped Fe ₂ O ₄ nanoparticles loaded on activated carbon	0.027	60.0	[32]
Alizarin Red and Purpurin dyes	Fe ₃ O ₄ magnetic nanoparticles	0.2	45.87 and 40.48	[33]
Benzene butyl phthalate	Multi-walled carbon nanotubes/Ag nanoparticles	1.2	87.8	[34]
Carcinogenic acid violet19 dye	Polyaniline-Fe ₂ O ₃ magnetic nanocomposite	0.5	62.44	[46]
Reactive Red 120 dye	<i>Albizia lebeck</i> fruit (pod)	0.05	1.68	[47]
Red 46 and Basic Yellow 28 dyes	Sorbent bentonite	0.4	45.87 and 40.48	[49]
Paraben dyes	<i>Origanum majorana</i> -AgNPs	0.05	93.0, 66.6 and 30.0	Present study

30.0, 66.6 and 93.0 mg g⁻¹ for methylparaben, ethylparaben and propylparaben dyes into *Origanum majorana*-AgNPs, respectively. Equilibrium adsorption showed that system followed Langmuir model. The kinetics scrutiny decided that paraben dyes deletion comply with pseudo-second-order rate equation. In addition the likelihood of recycling the adsorbent was well proved by desorption studies. Based on the results from the linear regression-based analysis, it was revealed that the derived empirical models represented a passable prediction of performance into *Origanum majorana*-AgNPs with significant determination coefficients ($R^2 = 0.994\text{--}0.984$). Additionally, the statistical outcomes guaranteed that the recommended equations could favorably be employed for the adsorption of paraben dyes from aqueous solutions. Further investigations on the suitability of this adsorbent for the deletion of other materials have been suggested. Also it was suggested to make inquiries about the suitability of this adsorbent in industrial application. The findings proved the appropriateness of the present procedure for the successful deletion of Pollutants from aqueous solution.

Acknowledgement

We would like to acknowledge our profound gratitude to the Islamic Azad University, Branch of Marvdash Iran for their partial support of this work.

References

- [1] D. Gryglik, M. Lach, J.S. Miller, The aqueous photosensitized degradation of butylparaben, *Photochem. Photobiol. Sci.*, 8 (2009) 549–555.
- [2] A. Prichodko, K. Jonusaite, V. Vickackaite, Hollow fibre liquid phase microextraction of parabens, *Cent. Eur. J. Chem.*, 7 (2009) 285–290.
- [3] D. Błędzka, D. Gryglik, J.S. Miller, Photodegradation of butylparaben in aqueous solutions by 254 nm irradiation, *J. Photochem. Photobiol., A*, 203 (2009) 131–136.
- [4] J. Regueiro, E. Becerril, C. Garcia-Jares, M. Llompert, Trace analysis of parabens, triclosan and related chlorophenols in water by headspace solid-phase microextraction with in situ derivatization and gas chromatography-tandem mass spectrometry, *J. Chromatogr.*, 1216 (2009) 4693–4702.
- [5] I. González-Mariño, J. Benito Quintana, I. Rodríguez, R. Cela, Simultaneous determination of parabens, triclosan and triclocarban in water by liquid chromatography/electrospray ionisation tandem mass spectrometry, *Rapid Commun. Mass Spectrom.*, 23 (2009) 1756–1766.
- [6] M. Chiara Pietrogrande, G. Basaglia, GC-MS analytical methods for the determination of personal-care products in water matrices, *TrAC, Trends Anal. Chem.*, 26 (2007) 1086–1094.
- [7] P. Canosa, I. Rodriguez, E. Rubi, N. Negreira, R. Cela, Formation of halogenated by-products of parabens in chlorinated water, *Anal. Chim. Acta*, 575 (2006) 106–113.
- [8] M. Masoudzadeh, N. Karachi, Enhanced removal of humic acids (HAs) from aqueous solutions using MWCNTs modified by N-(3-nitro-benzylidene)-N-trimethoxysilylpropyl-ethane-1, 2-diamine on equilibrium, thermodynamic and kinetics, *J. Phys. Theor. Chem.*, 14 (2017) 259–270.
- [9] S. Sheikhal, M. Emadi, N. Karachi, Adsorption kinetic and isotherm model studies for adsorption organic dyes by magnetic nanoparticles, *J. New Mater.*, 5 (2015) 29–42.
- [10] M. Masoudzadeh, N. Karachi, Removal of cadmium ion from waste water using carboxylated nanoporous graphene (G-COOH), *Eur. J. Anal. Chem.*, 13 (2018) em32, doi: 10.29333/ejac/90596.
- [11] S. Bagheri, H. Aghaei, M. Ghaedi, M. Monajjemi, K. Zare, Novel Au-Fe₃O₄ NPs loaded on activated carbon as a green and high efficient adsorbent for removal of dyes from aqueous solutions: application of ultrasound wave and optimization, *Eurasian J. Anal. Chem.*, 13 (2018) 1–10.
- [12] M.R. Parvizi, N. Karachi, Isotherm and kinetic study of disulfine blue and methyle orange dyes by adsorption onto by titanium dioxide-NPs loaded onto activated carbon: experimental design, *Orient. J. Chem.*, 33 (2017) 517–527.
- [13] H. Tajabadipour, M. Shahidi, N. Karachi, Polarization, EIS AND EN studies to evaluate the inhibition effect of vanillin as environment-friendly inhibitor on carbon steel in hydrochloric acid solution, *J. Phys. Theor. Chem.*, 10 (2014) 231–246.
- [14] B. Kakavandi, A. Raofi, S.M. Peyghambarzadeh, B. Ramavandi, M. Hazrati Niri, M. Ahmadi, Efficient adsorption of cobalt on chemical modified activated carbon: characterization, optimization and modeling studies. *Desal. Water Treatm.* 111 (2018) 310–321.
- [15] P. Nasehi, M. Saei Moghaddam, S.F. Abbaspour, N. Karachi, Preparation and characterization of a novel Mn-Fe₂O₄ nanoparticle loaded on activated carbon adsorbent for kinetic, thermodynamic and isotherm surveys of aluminum ion adsorption, *J. Sep. Sci. Technol.*, 55 (2019) 55162–55172.
- [16] S.H. Ahmadi, P. Davar, A. Manbohi, Adsorptive removal of Reactive Orange 122 from aqueous solutions by ionic liquid coated Fe₃O₄ magnetic nanoparticles as an efficient adsorbent, *Iran. J. Chem. Chem. Eng.*, 35 (2016) 63–73.
- [17] W.P. Utomo, E. Santoso, G. Yuhaneke, A.I. Triantini, M.R. Fatqi, M.F. Hudadan, N. Nurfitri, Studi Adsorpsi zat warna Naphthpl Yellow S pada limbah cair Menggunakan aktif dari ampas tebu, *Jurnal Kimia. (J. Chem.)*, 13 (2019) 104–116.
- [18] Z. Parsaee, N. Karachi, S.M. Abrishamifar, M.R. Rezaei Kahkha, R. Razavi, Silver-choline chloride modified graphene oxide: novel nano-bioelectrochemical sensor for Celecoxib detection and CCD-RSM model, *Ultrason. Sonochem.*, 45 (2018) 106–115.
- [18a] M. Sarafbidabad, Z. Parsaee, Z. Noor Mohammadi, N. Karachi, R. Razavi, Novel double layer film composed of reduced graphene oxide and Rose Bengal dye: design, fabrication and evaluation as an efficient chemosensor for silver(I) detection, *R. Soc. Chem.*, 16 (2018) 13674–13683.
- [19] N. Karachi, M. Hosseini, Z. Parsaee, R. Razavi, Novel high performance reduced graphene oxide based nanocatalyst decorated with Rh₂O₃/Rh-NPs for CO₂ photoreduction, *J. Photochem. Photobiol., A*, 364 (2018) 344–354.
- [20] Z. Parsaee, N. Karachi, R. Razavi, Ultrasound assisted fabrication of a novel optode base on a triazine based Schiff base immobilized on TEOS for copper detection, *Ultrason. Sonochem.*, 47 (2018) 36–46.
- [20a] N. Karachi, O. Azadi, R. Razavi, A. Tahvili, Z. Parsaee, Combinatorial experimental and DFT theoretical evaluation of a nano novel thio-dicarboxaldehyde based Schiff base supported on a thin polymer film as a chemosensor for Pb²⁺ detection, *J. Photochem. Photobiol. A*, 360 (2018) 152–165.
- [21] A.C. Burduşel, O. Gherasim, A.M. Grumezescu, L. Mogoantă, A. Fica, E. Andronescu, Biomedical applications of silver nanoparticles: an up-to-date overview, *Nanomaterials*, 8 (2018) 681, doi: 10.3390/nano8090681.
- [22] J.S. Justin Packia Jacob, A.N. Finub, Synthesis of silver nanoparticles using Piper longum leaf extracts and its cytotoxic activity against Hep-2 cell line, *Colloids Surf., B*, 91 (2012) 212–214.
- [23] G.H. Vatan Khah, A. Kohmareh, Enhanced removal of Bismark Brown (BB) dye from aqueous solutions using activated carbon from raw maize tassel: equilibrium, thermodynamic and kinetics, *J. Phys. Theor. Chem.*, 14 (2018) 237–249.
- [24] H.S. Ghazi Mokri, N. Modirshahla, M.A. Behnajady, B. Vahid, Adsorption of C.I. Acid Red 97 dye from aqueous solution onto walnut shell: kinetics, thermodynamics parameters, isotherms, *Int. J. Environ. Sci. Technol.*, 12 (2015) 1401–1408.
- [25] P.K. Singh, K. Bhardwaj, P. Dubey, A. Prabhune, UV-assisted size sampling and antibacterial screening of *Lantana camara* leaf extract synthesized silver nanoparticles, *RSC Adv.*, 5 (2015) 24513–24520.
- [26] Y.-H. Chen, C.-S. Yeh, A new approach for the formation of alloy nanoparticles: laser synthesis of gold–silver alloy from

- gold–silver colloidal mixtures: electronic supplementary information (ESI) available: experimental details, UV-VIS spectra, TEM images and EDX analysis for molar ratios (Au:Ag) of 1:2 and 2:1, *Chem. Commun.*, 4 (2001) 371–382.
- [27] C. Krishnaraj, E.G. Jagan, S. Jagan, P. Rajasekar, P.T. Selvakumar, N. Kalaichelvan, Synthesis of silver nanoparticles using *Acalypha indica* leaf extracts and its antibacterial activity against water borne pathogens, *Colloids Surf., B*, 76 (2010) 50–56.
- [28] M.D. Malinsky, K.L. Kelly, G.C. Schatz, R.P. Van Duyne, Chain length dependence and sensing capabilities of the localized surface plasmon resonance of silver nanoparticles chemically modified with alkanethiol self-assembled monolayers, *J. Am. Chem. Soc.*, 123 (2001) 1471–1482.
- [29] M. Ghaedi, B. Sadeghian, A.A. Pebdani, R. Sahraei, A. Daneshfar, C. Duran, Kinetics, thermodynamics and equilibrium evaluation of direct yellow 12 removal by adsorption onto silver nanoparticles loaded activated carbon, *Chem. Eng. J.*, 187 (2012) 133–141.
- [30] A.B. da Silva, J. Zanutto, M.T.A. Pietrobelli, Biosorption of reactive yellow dye by malt bagasse, *Adsorpt. Sci. Technol.*, 37 (2019) 236–259.
- [31] M.T. Ghaneian, M. Momtaz, M. Dehvari, An investigation of the efficacy of Cuttlefish bone powder in the removal of Reactive Blue 19 dye from aqueous solutions: equilibrium and isotherm studies, *J. Community Health Res.*, 1 (2012) 68–78.
- [32] M. Kiani, S. Bagheri, N. Karachi, E. Alipannahpour Dil, Adsorption of purpurin dye from industrial wastewater using Mn-doped Fe₂O₄ nanoparticles loaded on activated carbon, *Desal. Water Treat.*, 60 (2019) 1–8.
- [33] G. Absalan, A. Bananejad, M. Ghasemi, Removal of Alizarin Red and Purpurin from aqueous solutions using Fe₃O₄ magnetic nanoparticles, *Anal. Bioanal. Chem. Res.*, 4 (2017) 65–77.
- [34] S.H. Falahrodbari, Adsorption of benzene butyl phthalate with multi-walled carbon nanotubes/Ag nanoparticles and its applications, *Orient. J. Chem.*, 33 (2017) 910–919.
- [35] Y.S. Ho, G. McKay, The kinetics of sorption of divalent metal ions onto sphagnum moss peat, *Water Res.*, 34 (2000) 735–742.
- [36] S. Hajati, M. Ghaedi, H. Mazaheri, Removal of methylene blue from aqueous solution by walnut carbon: optimization using response surface methodology, *Desal. Water Treat.*, 57 (2016) 3179–3193.
- [37] S. Hajati, M. Ghaedi, B. Barazesh, F. Karimi, R. Sahraei, A. Daneshfar, A. Asghari, Application of high order derivative spectrophotometry to resolve the spectra overlap between BG and MB for the simultaneous determination of them: ruthenium nanoparticle loaded activated carbon as adsorbent, *J. Ind. Eng. Chem.*, 20 (2014) 2421–2427.
- [38] I. Langmuir, The adsorption of gases on plane surfaces of glass, mica and platinum, *J. Am. Chem. Soc.*, 40 (1918) 1361–1403.
- [39] H.M.F. Freundlich, Over the adsorption in solution, *J. Phys. Chem. A*, 57 (1906) 385–470.
- [40] M. Temkin, V. Levich, Adsorption equilibrium on heterogeneous surfaces, *J. Phys. Chem.*, 20 (1964) 1441.
- [41] M.M. Dubinin, The potential theory of adsorption of gases and vapors for adsorbents with energetically non-uniform surface, *Chem. Res.*, 60 (1960) 235–266.
- [42] M.M. Dubinin, Modern state of the theory of volume filling of micropore adsorbents during adsorption of gases and steams on carbon adsorbent, *Zh. Fiz. Khim.*, 39 (1965) 1305–1317.
- [43] M. Toor, B. Jin, Adsorption characteristics, isotherm, kinetics, and diffusion of modified natural bentonite for removing diazo dye, *Chem. Eng. J.*, 187 (2012) 79–88.
- [44] Y.S. Ho, Review of second-order models for adsorption systems, *J. Hazard. Mater.*, 136 (2006) 681–689.
- [45] F. Bouaziz, M. Koubaa, F. Kallel, R.E. Ghorbel, S.E. Chaabouni, Adsorptive removal of malachite green from aqueous solutions by almond gum: kinetic study and equilibrium isotherms, *J. Biol. Macromol.*, 105 (2017) 56–65.
- [46] R. Manohar, V.S. Shrivastava, Adsorption removal of carcinogenic acid violet 19 dye from aqueous solution by polyaniline-Fe₂O₃ magnetic nano-composite, *J. Mater. Environ. Sci.*, 6 (2015) 11–21.
- [47] G.H. Haghdoost, Removal of Reactive Red 120 from aqueous solutions using *Albizia lebbek* fruit (pod) partical as a low cost adsorbent, *J. Phys. Theor. Chem.*, 15 (2019) 141–148.
- [48] O.S. Bello, T.T. Siang, M.A. Ahmad, Adsorption of Remazol Brilliant Violet-5R reactive dye from aqueous solution by cocoa pod husk-based activated carbon: kinetic, equilibrium and thermodynamic studies, *Asia-Pac. J. Chem. Eng.*, 7 (2012) 378–388.
- [49] M. Turabik, Adsorption of basic dyes from single and binary component systems onto bentonite: Simultaneous analysis of Basic Red 46 and Basic Yellow 28 by first order derivative spectrophotometric analysis method, *J. Hazard. Mater.*, 158 (2008) 52–64.
- [50] P. Senthil Kumar, S. Ramalingam, C. Senthamarai, M. Niranjana, P. Vijayalakshmi, S. Sivanesan, Adsorption of dye from aqueous solution by cashew nut shell: studies on equilibrium isotherm, kinetics and thermodynamics of interactions, *Desalination*, 261 (2010) 52–60.